Chapter

Spark Plasma Sintered High-Entropy Alloys: An Advanced Material for Aerospace Applications

Ayodeji Ebenezer Afolabi, Abimbola Patricia I. Popoola and Olawale M. Popoola

Abstract

High-entropy alloys (HEAs) are materials of high property profiles with enhanced strength-to-weight ratios and high temperature-stress-fatigue capability as well as strong oxidation resistance strength. HEAs are multi-powder-based materials whose microstructural and mechanical properties rely strongly on stoichiometry combination of powders as well as the consolidation techniques. Spark plasma sintering (SPS) has a notable processing edge in processing HEAs due to its fast heating schedule at relatively lower temperature and short sintering time. Therefore, major challenges such as grain growth, porosity, and cracking normally encountered in conventional consolidation like casting are bypassed to produce HEAs with good densification. SPS parameters such as heating rate, temperature, pressure, and holding time can be utilized as design criteria in software like Minitab during design of experiment (DOE) to select a wide range of values at which the HEAs may be produced as well as to model the output data collected from mechanical characterization. In addition to this, the temperature-stress-fatigue response of developed HEAs can be analyzed using finite element analysis (FEA) to have an in-depth understanding of the detail of inter-atomic interactions that inform the inherent material properties.

Keywords: spark plasma sintering, high entropy alloys, advance material, aerospace application

1. Introduction

1.1 Background/motivation

In the aerospace industry, the landing gear is essential for support during landing and ground operations in an aircraft. Manufacturers attach the landing gear to primary structural members of an aircraft and must bear the heavy compressive load. Therefore, when landing, the impact energy of the aircraft will be absorbed through the design and a minimized load transmitted to the airframe. Thus, materials used for landing gear application must be able to withstand high operating temperatures, fatigue, creep, cyclic and translational movement of parts at high-speed,

and chemical, erosion, wear, and oxidation degradations [1–3]. The development of high-performance materials with superior characteristics for aerospace application has continually been the challenge faced by material engineers and scientists over the years. However, materials engineers constantly create and improve properties of materials by applying the existing knowledge of science to develop advanced engineering materials exhibiting better service performance through the development of various manufacturing techniques for different applications as shown in **Figure 1** [4–6]. The traditional alloys used for commercial purposes were designed by choosing a core element which made up the matrix of the part and addition of elemental solutes to the primary base element [7, 8]. This basic element, which made up the matrix, was primarily titanium [9–11], vanadium [12], iron [13], aluminum [14], or nickel [15], amongst others, produced for the aerospace industry with outstanding benefits. According to the conventional alloying system, each element compensates each other's deficiencies to give better properties of the alloy than to give the existence of the materials separately [16, 17]. However, the economy of the fabricated part with the conventional melting approach is the primary drive for research and development of powder metallurgy [18–21].

Landing gear components are typically manufactured with advanced materials using conventional metallic materials such as aluminum alloy 7075 [22–30], alloys steel 4340 [31–36], titanium 6Al-4V [37–42], titanium 6Al-6V-2Sn [43, 44], titanium 15Al-3Cr-3Al-3Sn [45–47], and titanium 10Al-2Fe-3V [48–52]. The most versatile titanium alloys in the aerospace industry are titanium 6Al-4V, titanium 6Al-6V-2Sn, titanium 15Al-3Cr-3Al-3Sn, and titanium 10Al-2Fe-3V because of their excellent properties. In the class of beta titanium alloys, Ti-15Al-3Cr-3Al-3Sn and Ti-10V-2Fe-3Al have been adopted for different airframe applications and landing operations [53]. The alloy Ti-10V-2Fe-3Al has the capability to substitute precipitation-hardening steels due to its in-depth hardenability and exceptional ductility. When it was successfully used in a Boeing 777 aerospace landing gear, the alloy Ti-10V-2Fe-3Al came to limelight. Initially, the alloy cost was higher than that of 4340 steel used in applications for landing gear [35]. However, the cost-benefit of using the alloy was achievable in the long run as the steel parts needed to be

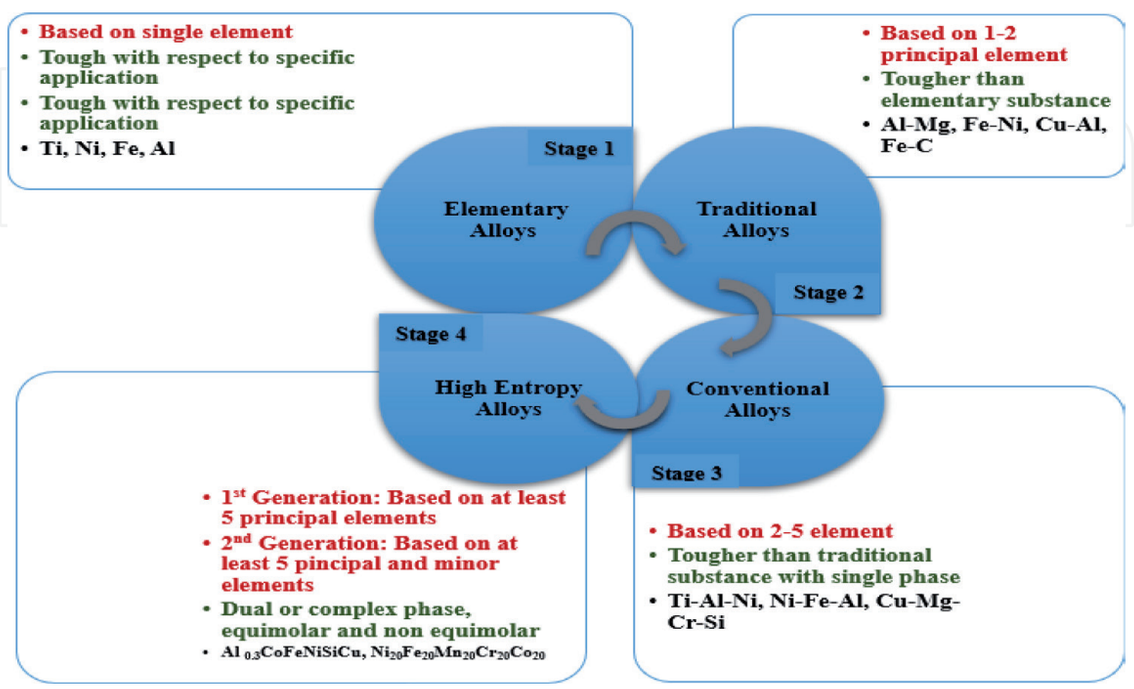

Figure 1.
The evolution and characteristics of alloys.

replaced due to potential susceptibility to stress corrosion cracking [54]. The alloy is therefore applied in many airframe applications of landing gear, wings, fuselage, doors, and cargo handling structures. Similarly, titanium alloys were not impressive for load-bearing components because of uneven stress distribution on parts during operation [55]. The nomenclature of typical landing gear is shown in **Figure 2**, comprising axie, shock, and drag strut, walking beam, and torsion links which are made up of Ti-10V-2Fe-3Al.

Ti-10V-2Fe-3Al popularly used in landing gear and slat/flap tracks was successfully fabricated using alloy forgings [56, 57]. Tracks are the dynamic beams allowing load transmission and movement between wings and moving slats. They are generally produced from maraging steel. Recently, Ti-10V-2Fe-3Al has been made of flap tracks fitted on the trailing side of the wings to perform similar functions. The total weight saving in Boeing 777 was about 40 kg by using six 5 ft. long flap tracks. The assessment of Ti-10V-2Fe-3Al's corrosion resistance is very important given its widespread use as structural parts that are susceptible to wear and corrosion in simulated environments through which an aircraft flies, which also makes the material not exceptional, and surface damage occurs in applications involving contact loading. In regard to this, Arya et al. [58] investigated the electrochemical corrosion performance of Ti-10V-2Fe-3Al alloy in different corrosive media namely, artificial seawater solution, Hank's solution, 0.5 M sulfuric acid, and 0.5 M hydrochloric acid solution. The authors used open circuit potential, current transient time, Tafel extrapolation potentiodynamic polarization curves, and electrochemical impedance spectroscopy to evaluate the corrosion rates. The results show that due to the formation of thick, compact, and stable passive film, this alloy has a lower corrosion rate in alkaline solution. Corrosion rate in acid solution is higher because the passive film is less compact, porous, and unstable. Li et al. [59] used a high-frequency push-pull fatigue testing machine to report the effect of fretting on the fatigue performance of Ti-6Al-4V and Ti-10V-2Fe-3Al alloys. For comparative analysis of the fretting effect on the fatigue performance of the different titanium alloy, the author obtained both plain and fretting fatigue curves. The result shows that Ti6Al4V titanium strength and plain fatigue are lower than Ti-10V-2Fe-3Al titanium strength. But the fretting fatigue of Ti6Al4V titanium is higher under each contact stress. The fatigue source depth of Ti-10V-2Fe-3Al alloy is greater than that of Ti6Al4V alloy. Hardening of Ti-10V-2Fe-3Al alloy is more serious after fretting. The wear mechanism of two titanium alloys is different; Ti1023 titanium alloy is more

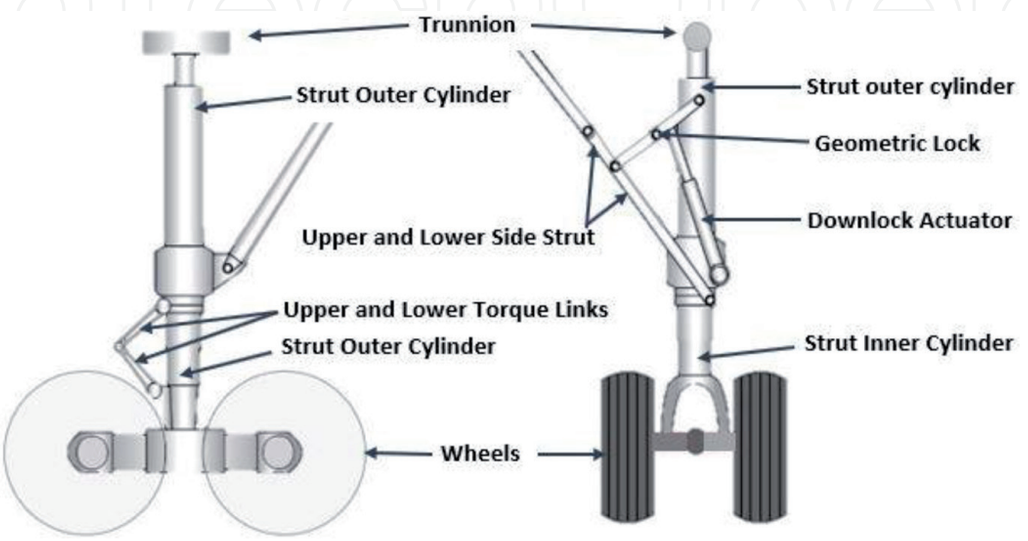

Figure 2.
The nomenclature of main landing gear bogie truck.

sensitive to fretting wear. According to Li et al. [60], the mechanical behavior of the Ti-10V-2Fe-3Al alloy under the high-temperature and dynamic loading conditions and the microscopic observations show that the microstructure of Ti-10V-2Fe-3Al alloy is sensitive to the external thermal loading. As the testing temperature is lower than the β phase transus, the β phase concentration almost remains unchanged besides a few of the refinement and spheroidize of β phase grains, which results in maintaining the high yield strength of the alloy. When the testing temperature is higher than the β phase transus, the thermal loading and mechanical loading can respectively cause various refinements and spheroidize of the β phase grain of alloy, which remarkably decreases the yield strength of the alloy. Based on the resulting stress and strain data obtained in simple shear, the high-temperature dynamic shear deformation mechanisms have been evaluated by using the characteristics of stress-strain behavior caused by thermal loading and mechanical loading. The high-temperature dynamic constitutive model is established based on the experimental results.

Utama et al. [61] reported surface height irregularities that occurred during machining Ti-10V-2Fe-3Al beta (β) titanium alloy. The author observed the height differences in two different regions, "soft region" and "hard region." The hard region has higher Fe and lower Al content, resulting in higher β-phase stability to resist the precipitation of the primary alpha (αp) phase caused by a solution treatment process failure. By contrast, a higher volume fraction of the αp phase and a lower volume fraction of the matrix consisted of a combination of β and secondary alpha (αs) phase.

A high number of αs/β interfaces in the matrix with a predicted 520 HV hardness resulted in harness improvement of the hard region. Hence, the hard and soft regions had different wear resistance capabilities during the machining process, resulting in surface height irregularities. Jiao et al. [62] reported that a complicated and unique phase transformation process takes place with forming different microstructures from forging and reconstruction method to study the spatial distribution of α phase in different grains present in the Ti-10V-2Fe-3Al alloy specimen. Since the process involves repeated heating and cooling during deposition, there was development of the complex and unique phase transformation process in the different microstructures. Their results showed plate-like morphology formation of α laths in the deposited alloy, and a tetrahedral relationship followed their precipitation from the β phase. The different orientation of the grain results in different specific morphologies. The α laths are perpendicular to each other when the cutting plane is parallel to the (100) plane of the BCC cell. If the cutting plane is parallel to the plane (111), a special morphology is established with a mixture of plate-like and rod-like phase α. Liu et al. [63] examined the evolution of microstructure and compression properties of Ti-10V-2Fe-3Al titanium alloy and solution treatments at temperatures ranging from 710 to 830°C, followed by treatment with aging. Ti-10V-2Fe-3Al alloys with α + β-phase have higher mechanical properties than single β-phase alloys. The content of the equiaxed α phase decreases with the increase in solution temperature. As a result, the alloy strength increases as the plasticity decreases. The highest yield strength value of 1668 MPa was obtained in the sample treated with a solution of 770°C treated for 2 hours, then water quenched and 520°C aging for 8 hours followed by air cooling. The stress-induced phase of martensite α" appeared in the sample solution treated at 830°C after dynamic compression of SHPB.

Tabachnikova et al. [64] measured the influence of temperature on Young's modulus for different structural states by mechanical resonance spectroscopy. The heat treatment of the samples led to an increase (~25%) of Young's modulus. Ren et al. [65] established that "Ti-10V-2Fe-3Al has the tendency to spall in a

brittle-ductile mixed fracture manner with very rough fracture surfaces covered by ductile dimples". The authors investigated the spall fracture behavior of a typical metastable β-titanium alloy, Ti-10V-2Fe-3Al, by subjecting it to shock loaded through a series of plate impact tests. The microstructural characteristics of the spall planes were systemically investigated for the influence of the shock-induced SIM phase transformation on the fracture behavior of the β-titanium alloy. The authors concluded that the spall strength of Ti-10V-2Fe-3Al is ca. 3.1 GPa at shock pressure below 8.5 GPa dropped by nearly 20% as the shock pressure exceeds 9 GPa due to the abundance of SIM phases with increased shock pressure. The microvoids in the spalled Ti-10V-2Fe-3Al mainly nucleate at the intersections of the grain boundary and the α martensite lath, which obviously showed that the shock-induced β-to-α martensite phase transformation strongly affected the spall fracture behavior of this alloy. The shock-induced β-to-α phase transformation has a detrimental effect on the spallation resistance of titanium alloys, which should be minimized in structural materials of titanium alloys that need to withstand shock wave loading. Srinivasu et al. [53] reported the presence of continuous grain boundary in Ti-10V-2Fe-3Al which is surrounded by a softer precipitate-free zone that leads to flow localization, thereby influencing fatigue crack propagation. The authors therefore studied the effect of processing and heat treatment on the tensile properties and fracture toughness of Ti-10V-2Fe-3Al, a high-strength metastable beta titanium alloy. The alloy was subsequently subjected to thermomechanical processing that included combinations of rolling and solution heat treatment in both α-β and β phase fields. The rolling temperatures ranged from 710°C (sub-transus) to 860°C (super-transus) and the temperatures of the solution treatment ranged from 710°C (sub-transus) to 830°C (super-transus). A systematic microstructural investigation (optical as well as scanning electron microscopy) was undertaken to correlate the property trends with the underlying microstructure, which is strongly dependent on the sequence of thermomechanical processing. A subtransus rolling followed by subtransus solution treatment resulted in a morphology being equiaxed while a super transus rolling followed by subtransus solution treatment resulted in a phase being more acicular/lenticular in morphology. While α-β rolling followed by α-β heat treatment gave better tensile properties, α-β heat treatment followed by β rolling resulted in superior fracture toughness.

In recent years, research has shown that advanced engineering materials used in industries are susceptible to corrosion and fatigue-related failures [66]. Authors attribute these challenges to design shortcomings, poor selection of materials, beyond the design limits, overloading, insufficient maintenance, and manufacturing defects [67]. The resulting repair and replacement costs take up almost half of the total budget; therefore, the performance of materials, particularly fatigue and corrosion resistances, has received widespread attention. According to Hemphill [68], the major drawback of this material is the formation of microcracks, which developed during fabrication as a manufacturing defect causing severe fatigue challenges. Current applications of Ti-10V-2Fe-3Al mainly in the wide range of aircraft structural components [69] are exceeding 200 flying components in each Boeing 777 alone [70, 71]. These applications were made by ingot metallurgy and forging [72], based on Boeing's original development for use in the Boeing 757 [73]. However, a primary problem with the process is the high buy-to-fly ratio [74], which results in about 90% scrap or a material utilization factor of just as much as 10%. Another issue is the severe segregation of α and β phases in the Ti-10V-2Fe-3Al as-cast ingot due to the presence of α and β stabilizers at 15 wt.%. This results in the so-called "beta flecks" in the forged microstructures [69].

Powder metallurgy (PM) allows the manufacture of near-net shape and effectively eliminates segregation by using micrometer-sized powder materials [69, 75].

There are many advantages of powder metallurgy compared to the conventional process in terms of fabricate titanium-based composite, low cost, full densification, no segregation, no inner defect, internal stress, excellent stability, and uniform microstructure. The high buy-to-fly ratio associated with many titanium components, combined with difficulties in forging and machining and recent availability issues, has resulted in a strong drive for near-net titanium manufacturing. PM [76]. is a very promising way to achieve this goal. Accordingly, a variety of PM-based techniques have been implemented to fabricate Ti-10V-2Fe-3Al using either pre-alloyed powder or titanium or TiH2 and master alloy powder blends [71, 77]. Generally, fully dense Ti-10V-2Fe-3Al alloy consolidated by hot isostatic pressing (HIP), or HIP + forging, with or without subsequent solid solution treatment and aging [78], can achieve tensile properties such as wrought alloys. Technically, the simplest and most attractive PM manufacturing route is the cold compaction and sinter approach [69]. Its potential for titanium manufacturing on a variety of titanium materials [79] has been well demonstrated. Although Ti-10V-2Fe-3Al's tensile properties were previously reported [80], the densification process, sintering mechanism, microstructural evolution during sintering, and their correlations with sintered mechanical properties were not given sufficient details. In contrast, the literature on powder-based titanium alloy manufacturing has focused largely on Ti-6Al-4V, with a focus on achieving full densification with respect to different manufacturing conditions [80, 81]. Therefore, there is an ultimate need to understand and establish the fundamentals of the cold-compaction-and-sinter PM approach for the fabrication of high strength or specialty solute rich titanium alloys such as Ti-10V-2Fe-3Al.

Spark plasma sintering (SPS) has been applied in the preparation of alloys, functional materials, ceramics, cermets, nanocomposites, and intermetallic compounds [82]. In recent times, extensive efforts were made towards research and development of SPS as a promising technique for high entropy alloys. Unlike conventional sintering methods, which usually use alternating heat current [83], SPS uses an on-off pulse current to heat the graphite die directly to complete the sintering process. Considering the SPS sintering mechanism, it is specifically assumed that an electrical field is formed between grains during sintering and high-temperature plasmas are excited under the action of pulse current to cause a cleaning effect on the surface of particles, leading to a sintering enhancement [84]. The spark plasma sintering method has several advantages over other conventional sintering techniques like hot pressing, mechanical alloying, and isostatic pressing due to high chances of sintering materials of near full densification and little grain growth [85]. SPS unique features also include a low heating profile, which makes it possible to sinter powders with controlled grain size and limited chemical interaction with other constituents [86]. The SPS method has proven its high effectiveness in fabricating ceramic composites and alloy materials for nano-applications, biomaterials, and electronic materials. From the traditional alloy design concept of titanium 10Al-2Fe-3V, however, HEAs are not based on a single element but on multi-component systems consisting of at least five main elements in an equal or near-equal atomic percentage (at.%) with no noticeable difference between the solute and the solvent [87]. According to existing physical metallurgy and phase diagrams, such multi-element alloys can produce many phases and intermetallic compounds, resulting in complex and fragile microstructures that are difficult to analyze and engineer but are likely to have finite practical values [88]. Experimental results indicate, beyond expectations, that the higher mixing entropy in these alloys enhances the formation of random solid-solution phases with simple structures such as face-centered cubic (FCC) structures [89], body-centered cubic (BCC) structures [90]), or hexagonal close packing (HCP) structures [91], thereby

reducing the number of phases [89, 92, 93]. The new alloy design strategy has since opened up an enormous, unexplored multi-component alloy field. The alloy design strategy has achieved unimaginable successes, and great efforts have been devoted to the development and application of many HEAs [94], in various fields because of their excellent performance, such as unique wear resistance [95], excellent strength and thermal stability at elevated temperatures [96], superior high elongation [93], high fatigue, and fracture toughness [97]. Han et al. [98] showed that the "addition of Ti is beneficial to the strength and the compressive ductility of the HEAs at room temperature". The authors presented a new refractory HEA alloy of TiNbMoTaW fabricated from addition of Ti to NbMoTaW alloy. The new TiNbMoTaW HEA was found to have a BBC phase structure that can be maintained even after 24-hour annealing at 1200°C. The room temperature yield strengths and compressive plastic strains of the developed TiNbMoTaW and TiVNbMoTaW HEAs have been significantly enhanced in comparison with the mechanical performance of HEAs NbMoTaW and VNbMoTaW. Also, with impressive yield strengths of ~586 and ~659 MPa at 1200°C, the TiNbMoTaW and TiVNbMoTaW HEAs showed very promising high-temperature strength. As a result of these property profiles, it was suggested that the newly developed TiNbMoTaW and TiVNbMoTaW HEAs have potentials in applications of high-temperature structural materials.

Consequently, extensive research has been conducted to develop next-generation aerospace materials with high mechanical performance and superior corrosion resistance to achieve improvements in both performance and cost repetition. For traditional alloys, one or two principal components are selected based on a specific property requirement, and other alloying components are added to further improve their properties because of the huge formation of bulk intermetallic compounds which occurred as a result of the atomic ratios of elements reaching a 40% mark and above. Thus, this depletes the reliability of the alloy during service. Therefore, the search for an alloy with atomic ratios lower than 35% commenced in 1996 [99]. Hence, the possibility of combining several metallic principal elements in equal atomic compositions was explored and it was named high-entropy alloys (HEAs). HEAs always have the combination of at least five principal elements, each with an atomic percentage (at. %) between 5 and 35%. Generally, the atomic percentage of each minor element, if present at all, is always smaller than 5. The definition is expressed as follows in Eqs. (1) and (2) [94, 102]:

$$n_{major} \geq 5,5at.\% \leq c_i \leq at35at.\% \tag{1}$$

$$n_{minor} \geq 0, c_j 5at.\% \tag{2}$$

where n_{major} represents the major elements, n_{minor} represents the minor elements, c_i represents the atomic percentages of the major element, and c_j represents the atomic percentages of the minor element.

This definition shows that HEAs need not to be equimolar or near-equimolar, and even contain minor elements to balance various material properties [100]. HEAs can easily be formed into simple FCC phase structures [101], BCC [102], and HCP [91] solid-solution structures. One renowned HEA is an equimolar-shaped Cantor alloy [102] consisting of Fe (BCC), Co (HCP), Cr (BCC), Mn (BCC), and Ni (FCC), with a solid-solution FCC phase when dendritically cooled in the as-shaped sample. Then, by adding Cu (FCC), Nb (FCC), or V (BCC), the five-component alloy was extended to a six-component alloy system, showing the simple solid-solution FCC structure in the as-cast alloy with different lattice parameters. When the HCP type Ti was added, a solid-solution phase of the FCC formed a BCC

structure [103]. Another typical example is the AlxCoCrFeNi (molar percentage, $2 \geq x \geq 0$) system prepared by arc melting [104]. The CoCrFeNi as-cast alloy has a solid-solution phase of pure FCC. The AlxCoCrFeNi system changes the crystal structure from FCC to FCC + BCC phases by increasing the Al molar percentage from 0 to 2 and finally to a single BCC phase [104]. A typical TaNbHfZr alloy has a structure with only BCC [105].

Alloy design is a novel means of maximizing and synergizing metal counterparts in HEA multi-material systems. The design encompasses several considerations such as atomic radius, solid solution solubility, powder stoichiometry, processing technique, and the processing conditions or parameters chosen. Thus, HEAs possess dynamic and exceptional properties, such as high hardness and strength profiles, good oxidation and corrosion resistance, and high-temperature softening resistance, which are crucial in prospective engineering applications. HEAs fabricated by SPS have been reported to possess excellent densification properties, as well as high strength and hardness profile. Mohanty et al. [106] research output on a multicomponent equiatomic AlCoCrFeNi high entropy alloy developed by spark plasma sintering established a high mechanical strength. The sintered samples at the optimum temperature of 1273 K displayed the highest microhardness. Fang et al. [85] also researched the mechanical behavior of $Al_{0.5}CrFeNiCo_{0.3}C_{0.2}$ high entropy alloy. They recorded a compressive strength of 2131 MPa and a Vickers microhardness of 617 HV of the $Al_{0.5}CrFeNiCo_{0.3}C_{0.2}$ high entropy alloy. Zhao et al. [107] fabricated HEAs on a carbon steel substrate via spark plasma sintering, which are considered as excellent coating materials due to their high hardness, good wear, and corrosion resistance. The microstructure evolved from FCC to FCC + BCC mixed structure. $Al_xCrFeCoNiCu$ (x = 0, 1, 2, 3) coating has an average hardness of approximately 682 $HV_{0.2}$, which is the highest hardness in all the HEA coatings. Compared with AISI 52100 steel, spark plasma sintered Al2CrFeCoNiCu and Al3Cr-FeCoNiCu HEA coatings show exceptional sliding wear resistance and extremely low friction coefficient in comparison with AISI 52100 steel. Al3CrFeCoNiCu HEA coating wear resistance is approximately four times better than that of bearing steel, showing a promising application as a wear-resistant material According to Chen et al. [108], research outputs of several literature studies indicate that the addition of Ni to Ti-10V-2Fe-3Al is beneficial to the improved mechanical performances of the HEA, making the HEA a good material for high-temperature applications. Nickel is the fifth most common element on earth's crust. As a high-profile element with a good property suited for diverse applications especially that of the aerospace industry, there is no substitute for Ni without reducing performance or increasing cost. The biggest use of nickel is in alloying, particularly with chromium and other metals to produce stainless and heat-resisting steels constituting 65% production [109]. Another 20% is mostly used for highly specialized industrial, aerospace, and military applications. With characteristic melting point of 1453°C, Ni has reliable corrosion and oxidation properties, and readily forms alloys [110, 111].

Chromium, on the other hand, is generally used in metallurgy to impart corrosion resistance, and it also has good strengthening effect of forming stable metal carbides at the grain boundaries of its alloying counterpart [112, 113]. Chromium has excellent mechanical properties such as high corrosion and wear resistance. Therefore, in alloying, it finds a good match with Ni to form Ni-Cr alloys when used with Ti-10V-2Fe-3Al for making landing gear, wind turbine, engine components, and many other industrial and mechanical components where high wear-resistance is needed such as in aerospace applications. The structure of Ni-Cr alloys depends on the percentage composition of nickel or chromium, and the temperature. It is noteworthy that Ni-Cr alloys will be dominated by the π phase, which tends to be

brittle at about 60–75% Ni addition. The crystal structure of the FCC is found in the γ phase, and the γ phase shows improved strength and ductility in comparison with the σ phase. The FCC crystal structure is commonly found in Ni-rich alloys, while the BCC crystal structure tends to be found in Cr-rich alloys. The γ phase Ni-Cr alloy can be converted into the ε phase at high pressures, which shows an HCP crystal structure. The alloying element helps stabilize the BCC structure of Ti-10V-2Fe-3Al HEA, increasing the hardness and plastic strain of the alloy. However, there are limited publications in the literature on Ti-10V-2Fe-3Al alloy with Ni and Cr additions, despite the different manufacturing routes that had been established. Moreover, reports investigating the fatigue, corrosion, and oxidation behaviors of spark plasma sintered Ti-10V-2Fe-3Al-Ni-Cr HEAs with their potential applications are scarce. Therefore, this work proposes to use the spark plasma sintering manufacturing technique to synthesize novel Ti-10V-2Fe-3Al-Ni, Ti-10V-2Fe-3Al-Cr, Ti-10V-2Fe-3Al-Ni-Cr, and Ti-V-Fe-Al-Ni-Cr high entropy alloys (HEAs) for making landing gear. Thereafter, the synthesized alloys will be characterized in terms of microstructure, composition, and phase transformation using optical microscopy (OM), X-ray diffraction (XRD), and scanning electron microscopy (SEM) with energy-dispersive X-ray spectroscopy (EDX), respectively. Also, the mechanical and electrochemical properties of the materials will be carried out, and the effects of temperature and stress distributions of the high entropy alloy material during the SPS process will be modeled.

2. Conclusion

From the open literature above, the authors agreed that the current market material (Ti-10V-2Fe-3Al) used in high-temperature applications such as gas turbine and turbine engine in the aerospace industry experience several failures such as high-temperature oxidation and corrosion, limited hardness, and wear resistance. It is confirmed that spark plasma sintering is a potential way to fabricate HEAs which possess properties such as improved microhardness, compressive/tensile strength, tribology, thermal properties, and corrosion resistance properties for low and high-temperature applications as generally agreed by all the authors. Also, it is generally accepted by the authors that SPS processing parameters play a significant role in the mechanical properties of the final developed alloys. The authors concluded that HEAs are the potential replacement for nickel-based superalloys in high-temperature applications. Furthermore, the authors agreed that it is possible to simulate the SPS process by means of finite element modeling. However, SPS simulation of thermal distribution and stress distribution analysis for the development of HEAs are limited in the open literature. Thus, this paper exposes the influence of spark plasma sintering parameters on the mechanical properties of the synthesized alloy.

Author details

Ayodeji Ebenezer Afolabi[1], Abimbola Patricia I. Popoola[1*] and Olawale M. Popoola[2]

1 Department of Chemical, Metallurgical and Materials Engineering, Tshwane University of Technology, Pretoria, South Africa

2 Centre for Energy and Electric Power, Tshwane University of Technology, Pretoria, South Africa

*Address all correspondence to: popoolaap@tut.ac.za

IntechOpen

References

[1] Krüger W. Design and simulation of semi-active landing gears for transport aircraft. Mechanics of Structures and Machines. 2002;**30**(4):493-526

[2] Sivaranjani T, Kumar DP, Manjunatha CM, Manjuprasad M. Fatigue life estimation of typical fighter aircraft main landing gear using finite element analysis. In: Advances in Structural Integrity. Singapore: Springer; 2018. pp. 39-52

[3] Saraç H. Shock Absorption Technology for Landing Gears; 2018

[4] Zhang W, Liaw PK, Zhang Y. Science and technology in high-entropy alloys. Science China Materials. 2018;**61**(1):2-22

[5] Adesina O, Popoola P, Fatoba O. Laser surface modification—A focus on the wear degradation of titanium alloy. In: Fiber Laser. IntechOpen.; 2016;**16**:368-381

[6] Dutta S, Robi PS. 5 ChAPtEr Development in materials for sustainable manufacturing. Sustainable Material Forming and Joining. New York: Taylor & Francis Group LLc, London; 2019

[7] Chikumba S, Rao VV. High entropy alloys: Development and applications. In: Proceedings of the 7th International Conference on Latest Trends in Engineering & Technology (ICLTET' 2015); Irene, Pretoria. 2015

[8] Tsao L, Chang S, Yu Y. Direct active soldering of Al 0.3 CrFe 1.5 MnNi 0.5 high entropy alloy to 6061-Al using Sn-Ag-Ti active solder. Transactions of Nonferrous Metals Society of China. 2018;**28**(4):748-756

[9] Jindal P, Worcester F, Walia K, Gupta A, Breedon P. Finite element analysis of titanium alloy-graphene based mandible plate. Computer methods in biomechanics and biomedical engineering. 2019;**22**(3):324-330

[10] Smyrnova KV, Pogrebnjak AD, Kassenova LG. Structural features and properties of biocompatible Ti-based alloys with β-stabilizing elements. In: Advances in Thin Films, Nanostructured Materials, and Coatings. Singapore: Springer; 2019. pp. 319-330

[11] Geetha M, Singh AK, Asokamani R, Gogia AK. Ti based biomaterials, the ultimate choice for orthopaedic implants—A review. Progress in Materials Science. 2009;**54**(3):397-425

[12] Chu Q, Zhang M, Li J, Yan C, Qin Z. Influence of vanadium filler on the properties of titanium and steel TIG welded joints. Journal of Materials Processing Technology. 2017;**240**:293-304

[13] Schinhammer M, Hänzi AC, Löffler JF, Uggowitzer PJ. Design strategy for biodegradable Fe-based alloys for medical applications. Acta Biomaterialia. 2010;**6**(5):1705-1713

[14] Dobrzański LA, Matula G, Dobrzańska-Danikiewicz AD, Malara P, Kremzer M, Tomiczek B, et al. Composite materials infiltrated by aluminium alloys based on porous skeletons from alumina, mullite and titanium produced by powder metallurgy techniques. In: Powder Metallurgy-Fundamentals and Case Studies. IntechOpen.; 2017

[15] Han G, Sato K, Ueno T, Chiba A. Method for manufacturing Ni-based super-heat-resistant alloy. US Patent App. 15/548,447; 2019

[16] Doorbar PJ, Kyle-Henney S. 4.19 Development of Continuously-Reinforced Metal Matrix Composites for Aerospace Applications; 2018

[17] Prasad YV, Rao KP, Sasidhar S, editors. Hot Working Guide: A Compendium of Processing Maps. Ohio, USA: ASM International; 2015

[18] Fang ZZ, Paramore JD, Sun P, Chandran KR, Zhang Y, Xia Y, et al. Powder metallurgy of titanium-past, present, and future. International Materials Reviews. 2018;**63**(7):407-459

[19] Huang R, Riddle M, Graziano D, Warren J, Das S, Nimbalkar S, et al. Energy and emissions saving potential of additive manufacturing: The case of lightweight aircraft components. Journal of Cleaner Production. 2016;**135**:1559-1570

[20] Fang ZZ, Sun P. Pathways to optimize performance/cost ratio of powder metallurgy titanium-a perspective. Key Engineering Materials. 2012;**520**:15-23

[21] Seong S, Younossi O, Goldsmith BW. Titanium: Industrial Base, Price Trends, and Technology Initiatives. Santa Monica, CA: Rand Corporation; 2009

[22] Al-Bahkali EA. Analysis of different designed landing gears for a light aircraft. World Academy of Science, Engineering and Technology. International Journal of Mechanical, Aerospace, Industrial, Mechatronic and Manufacturing Engineering. 2013;7(7):1333-1336

[23] Zhu L, Li N, Childs P. Light-weighting in aerospace component and system design. Propulsion and Power Research. 2018;7(2):103-119

[24] Kaya H, Uccedil M, Cengiz A, Erguuml RE. The effect of aging on the machinability of AA7075 aluminium alloy. Scientific Research and Essays. 2012;7(27):2424-2430

[25] Mahajan Y, Peshwe D. Effect of temper conditions on abrasive Wear behavior of AA7010 alloy. Transactions of the Indian Institute of Metals. 2018;**71**(4):1025-1032

[26] Yildirim M, Özyürek D, Gürü M. The effects of precipitate size on the hardness and wear behaviors of aged 7075 aluminum alloys produced by powder metallurgy route. Arabian Journal for Science and Engineering. 2016;**41**(11):4273-4281

[27] Senthil K, Iqbal M, Chandel P, Gupta N. Study of the constitutive behavior of 7075-T651 aluminum alloy. International Journal of Impact Engineering. 2017;**108**:171-190

[28] Neves RS, Silva DP, Motheo AJ. Corrosion protection of AA7075 aluminium alloy by trimethoxy-silanes self-assembled monolayers. ISRN Electrochemistry. 2013;**2013**:142493

[29] Arriscorreta CA. Statistical Modeling for the Corrosion Fatigue of Aluminum Alloys 7075-T6 and 2024-T3. The University of Utah; 2012

[30] Martín M, Cano M, Castillo G, Herrera M, Martín F. Influence of milling parameters on mechanical properties of AA7075 aluminum under corrosion conditions. Materials. 2018;**11**(9):1751

[31] Yunaidi Y. Pengaruh Jumlah Konsentrasi Larutan Garam Pada Proses Quenching Baja Karbon Sedang S45C. Jurnal Mekanika dan Sistem Termal. 2016;**1**(3):70-76

[32] Ritchie RO, Francis B, Server WL. Evaluation of toughness in AISI 4340 alloy steel austenitized at low and high temperatures. Metallurgical Transactions A. 1976;7(6):831-838

[33] Banerjee B. The mechanical threshold stress model for various tempers of AISI 4340 steel. International Journal of Solids and Structures. 2007;**44**(3-4):834-859

[34] Lee W-S, Su T-T. Mechanical properties and microstructural features of AISI 4340 high-strength alloy steel under quenched and tempered conditions. Journal of Materials Processing Technology. 1999;**87**(1-3):198-206

[35] Braga C, dSilva LR, Barbosa EJA, Corrêa ECS. Surface integrity characterization of hardened AISI 4340 steel in grinding process with biodegradable formulations of cutting fluids. Materials Research. 2017;**20**(2):496-501

[36] Zhou J, Retraint D, Sun Z, Kanouté P. Comparative study of the effects of surface mechanical attrition treatment and conventional shot peening on low cycle fatigue of a 316L stainless steel. Surface and Coatings Technology. 2018;**349**:556-566

[37] Ugarte A, M'Saoubi R, Garay A, Arrazola P. Machining behaviour of Ti-6Al-4 V and Ti-5553 Allooys in interrupted cutting with PVD coated cemented carbide. Procedia CIRP. 2012;**1**:202-207

[38] Raghavendra M, Ramachandra C, Srinivas T, Pai MP. Optimization of surface roughness in turning operation in machining of TI-6AL-4V (titanium grade-5). In: IOP Conference Series: Materials Science and Engineering. IOP Publishing; 2018

[39] Antunes RA, Salvador CAF, d Oliveira MCL. Materials selection of optimized titanium alloys for aircraft applications. Materials Research. 2018;**21**(2):1-9

[40] Sterling A, Shamsaei N, Torries B, Thompson SM. Fatigue behaviour of additively manufactured Ti-6Al-4 V. Procedia Engineering. 2015;**133**:576-589

[41] Ritchie RO, Francis B, Server WL. High-cycle fatigue of Ti-6Al-4V. Fatigue and Fracture of Engineering Materials and Structures. 1999;**22**(7):621-632

[42] Razavi S, Bordonaro G, Ferro P, Torgersen J, Berto F. Fatigue behavior of porous Ti-6Al-4V made by laser-engineered net shaping. Materials. 2018;**11**(2):284

[43] Kinney JR. The Power for Flight: NASA's Contributions to Aircraft Propulsion. Vol. 631. Washington, DC: Government Printing Office; 2018

[44] Amateau MF, Kendall EG. A Review of Ti-6A1-6V-2Sn Fatigue Behavior. Aerospace Corp el Segundo ca Materials Sciences Lab; 1970

[45] Maurotto A, Siemers C, Muhammad R, Roy A, Silberschmidt V. Ti alloy with enhanced machinability in UAT turning. Metallurgical and Materials Transactions A. 2014;**45**(6):2768-2775

[46] Demiral M, Nowag K, Roy A, Ghisleni R, Michler J, Silberschmidt VV. Enhanced gradient crystal-plasticity study of size effects in a β-titanium alloy. Modelling and Simulation in Materials Science and Engineering. 2017;**25**(3):035013

[47] Demiral M. Enhanced Gradient Crystal-Plasticity Study of Size Effects in BCC Metal; 2012

[48] Furuhara T, Maki T, Annaka S. Superelasticity in β titanium alloys with nitrogen addition. Journal of Materials Engineering and Performance. 2005;**14**(6):761-764

[49] Quan G, Pu S, Wen H, Zou Z, Zhou J. Quantitative analysis of dynamic softening behaviors induced by dynamic recrystallization for Ti-10V-2Fe-2Al alloy. High Temperature Materials and Processes. 2015;**34**(6):549-561

[50] Yang R, Pan Y, Chen W, Sun Q, Xiao L, Sun J. Deformation behavior

and the mechanism of micro-scale Ti-10V-2Fe-3Al pillarsin compression. Acta Metallurgica Sinica. 2015;**52**(2):135-142

[51] Forged I. Mechanical-Property Data Ti-10V-2Fe-3AI Alloy. Columbus, Ohio: Air Force Wright Aeronautical Laboratory, Materials Laboratory F33615-80-C-5168. 1982

[52] Liu J, Sun J, Chen W. Surface integrity of TB6 titanium alloy after dry milling with solid carbide cutters of different geometriy. The International Journal of Advanced Manufacturing Technology. 2017;**92**(9-12):4183-4198

[53] Srinivasu G, Natraj Y, Bhattacharjee A, Nandy T, Rao GN. Tensile and fracture toughness of high strength β titanium alloy, Ti-10V-2Fe-3Al, as a function of rolling and solution treatment temperatures. Materials & Design. 2013;**47**:323-330

[54] Rocha-Reséndez R, Cabral-Miramontes J, Gaona-Tiburcio C, Zambrano-Robledo P, Estupiñan-López F, Calderon FA. Corrosion behavior of austempered ductile iron used in the aeronautical industry evaluated on acid solutions. In: International Materials Research Congress. Springer; 2016

[55] Cui C, Hu B, Zhao L, Liu S. Titanium alloy production technology, market prospects and industry development. Materials & Design. 2011;**32**(3):1684-1691

[56] Jackson M, Dashwood R, Flower H, Christodoulou L. The microstructural evolution of near beta alloy Ti-10V-2Fe-3Al during subtransus forging. Metallurgical and Materials Transactions A. 2005;**36**(5):1317-1327

[57] Jackson M, Jones N, Dye D, Dashwood R. Effect of initial microstructure on plastic flow behaviour during isothermal forging of Ti-10V-2Fe-3Al. Materials Science and Engineering A. 2009;**501**(1-2):248-254

[58] Arya SB, Bhattacharjee A, Roy M. Electrochemical corrosion behavior of Ti-10V-2Fe-3Al in different corrosive media. Materials and Corrosion. 2018;**69**(8):1025-1038

[59] Li ZY, Liu XL, Wu GQ, Huang Z. Fretting fatigue behavior of Ti-6Al-4V and Ti-10V-2Fe-3Al alloys. Metals and Materials International. 2019;**25**(1):64-70

[60] Li L, Zhang X, Li Z, Wang Z, Ma W. The mechanical behaviours of the Ti-10V-2Fe-3Al alloy under the high-temperature and dynamic loading conditions. In: EPJ Web of Conferences. EDP Sciences; 2018

[61] Utama MI, Ammar AA, Park N, Baek ER. Origin of surface irregularities on Ti-10V-2Fe-3Al Beta titanium alloy. Metals and Materials International. 2018;**24**(2):291-299

[62] Jiao Z, Fu J, Li Z, Cheng X, Tang H, Wang H. The spatial distribution of α phase in laser melting deposition additive manufactured Ti-10V-2Fe-3Al alloy. Materials & Design. 2018;**154**:108-116

[63] Liu AJ, Wang L, Dai HX. Effect of heat treatment on the microstructure and dynamic behavior of Ti-10V-2Fe-3Al alloy. Materials Science Forum. 2018;**910**:155-160

[64] Tabachnikova E, Laktionova M, Semerenko YA, Shumilin S, Podolskiy A, Tikhonovsky M, et al. Mechanical properties of the high-entropy alloy Al0. 5CoCrCuFeNi in various structural states at temperatures of 0.5-300 K. Low Temperature Physics. 2017;**43**(9):1108-1118

[65] Ren Y, Xue Z, Yu X, Tan C, Wang F, Cai H. Spall strength and fracture behavior of Ti–10V–2Fe–3Al alloy

during one-dimensional shock loading. International Journal of Impact Engineering. 2018;**111**:77-84

[66] Xu L, Chen H, Shen L, Che X, Wang Q, Fu Z. Study on fatigue crack propagation behavior in corrosion environment of a cold-rolled austenitic stainless steel. Corrosion. 2017;**73**(8):961-969

[67] Maleque MA, Salit MS. Materials Selection and Design. Singapore: Springer; 2013

[68] Hemphill EA. Fatigue behavior of Al0. 5CoCrCuFeNi high entropy alloys. Acta Materialia. 2012;**60**(16):5723-5734

[69] Yang Y, Luo S, Schaffer G, Qian M. Sintering of Ti–10V–2Fe–3Al and mechanical properties. Materials Science and Engineering A. 2011;**528**(22-23):6719-6726

[70] Boyer RR. Aerospace applications of beta titanium alloys. Journal of Management. 1994;**46**(7):20-23

[71] Welsch G, Boyer R, Collings EW, editors. Materials Properties Handbook: Titanium Alloys. Ohio, USA: ASM International; 1993

[72] Bhattacharjee A, Bhargava S, Varma V, Kamat S, Gogia A. Effect of β grain size on stress induced martensitic transformation in β solution treated Ti–10V–2Fe–3Al alloy. Scripta Materialia. 2005;**53**(2):195-200

[73] Ashley S. Boeing 777 gets a boost from titanium. Mechanical Engineering. 1993;**115**(7):60

[74] Barnes JE, Peter W, Blue CA. Evaluation of low cost titanium alloy products. Materials Science Forum. 2009;**618-619**:165-168

[75] Criswell D. Powder metallurgy in space manufacturing. In: 4th Space Manufacturing; Proceedings of the Fifth Conference. 1980

[76] Boyer RR, Williams JC, Wu X, Clark LP. A realistic approach for qualification of PM applications in the aerospace industry. In: Titanium Powder Metallurgy. Butterworth-Heinemann: Elsevier; 2015. pp. 497-514

[77] Samal P, Newkirk J. Properties and Selection of Powder Metallurgy Titanium and its Alloys Asminternational, Materials Park OH; 2015

[78] Perevoshchikova N, Hutchinson C, Wu X. The design of hot-isostatic pressing schemes for Ti–5Al–5Mo–5V–3Cr (Ti-5553). Materials Science and Engineering A. 2016;**657**:371-382

[79] Luo S, Yan M, Schaffer G, Qian M. Sintering of titanium in vacuum by microwave radiation. Metallurgical and Materials Transactions A. 2011;**42**(8):2466

[80] Agarwal G, Dongare AM. Modeling the thermodynamic behavior and shock response of Ti systems at the atomic scales and the mesoscales. Journal of Materials Science. 2017;**52**:10853-10870

[81] Zhao Y, Li R, Mo J, Tan F, Sun Y. Experimental study on spallation of titanium alloy plates under intense impulse loading. In: Multidisciplinary Digital Publishing Institute Proceedings. 2018

[82] Fu Z, Chen W, Fang S, Zhang D, Xiao H, Zhu D. Alloying behavior and deformation twinning in a CoNiFeCrAl0.6Ti0.4 high entropy alloy processed by spark plasma sintering. Journal of Alloys and Compounds. 2013;**553**:316-323

[83] Pradhan SK, Kalidoss J, Barik R, Sivaiah B, Dhar A, Bajpai S. Development of high density

tungsten based scandate by spark plasma sintering for the application in microwave tube devices. International Journal of Refractory Metals and Hard Materials. 2016;**61**:215-224

[84] Liu Y, Wang J, Fang Q, Liu B, Wu Y, Chen S. Preparation of superfine-grained high entropy alloy by spark plasma sintering gas atomized powder. Intermetallics. 2016;**68**:16-22

[85] Fang S, Chen W, Fu Z. Microstructure and mechanical properties of twinned Al0. 5CrFeNiCo0. 3C0. 2 high entropy alloy processed by mechanical alloying and spark plasma sintering. Materials & Design. 2014;**54**:973-979

[86] Fu Z, Chen W, Wen H, Chen Z, Lavernia EJ. Effects of Co and sintering method on microstructure and mechanical behavior of a high-entropy Al0. 6NiFeCrCo alloy prepared by powder metallurgy. Journal of Alloys and Compounds. 2015;**646**:175-182

[87] Yeh JW, Chen SK, Lin SJ, Gan JY, Chin TS, Shun TT, et al. Nanostructured high-entropy alloys with multiple principal elements: Novel alloy design concepts and outcomes. Advanced Engineering Materials. 2004;**6**(5):299-303

[88] Yeh JW, Chen YL, Lin SJ, Chen SK. High-entropy alloys-a new era of exploitation. Materials Science Forum. 2007;**560**:1-9

[89] Miracle DB, Senkov O. A critical review of high entropy alloys and related concepts. Acta Materialia. 2017;**122**:448-511

[90] Sharma A, Deshmukh SA, Liaw PK, Balasubramanian G. Crystallization kinetics in AlxCrCoFeNi ($0 \leq x \leq 40$) high-entropy alloys. Scripta Materialia. 2017;**141**:54-57

[91] Zhao Y, Qiao J, Ma S, Gao M, Yang H, Chen M, et al. A hexagonal close-packed high-entropy alloy: The effect of entropy. Materials & Design. 2016;**96**:10-15

[92] Miracle D, Senkov O. A Critical Review of High Entropy Alloys and Related Concepts (Postprint). Dayton, OH, United States: UES INC; 2016

[93] Li Z, Tasan CC, Pradeep KG, Raabe D. A TRIP-assisted dual-phase high-entropy alloy: Grain size and phase fraction effects on deformation behavior. Acta Materialia. 2017;**131**:323-335

[94] Pickering E, Jones N. High-entropy alloys: A critical assessment of their founding principles and future prospects. International Materials Reviews. 2016;**61**(3):183-202

[95] Chuang M-H, Tsai M-H, Wang W-R, Lin S-J, Yeh J-W. Microstructure and wear behavior of AlxCo1. 5CrFeNi1. 5Tiy high-entropy alloys. Acta Materialia. 2011;**59**(16):6308-6317

[96] Zou Y, Ma H, Spolenak R. Ultrastrong ductile and stable high-entropy alloys at small scales. Nature Communications. 2015;**6**:7748

[97] Gludovatz B, Hohenwarter A, Catoor D, Chang EH, George EP, Ritchie RO. A fracture-resistant high-entropy alloy for cryogenic applications. Science. 2014;**345**(6201):1153-1158

[98] Han Z, Chen N, Zhao S, Fan L, Yang G, Shao Y, et al. Effect of Ti additions on mechanical properties of NbMoTaW and VNbMoTaW refractory high entropy alloys. Intermetallics. 2017;**84**:153-157

[99] Aristeidakis IS, Tzini MIT. High Entropy Alloys; 2016

[100] He JY, Wang H, Huang HL, Xu XD, Chen MW, Wu Y, et al. A precipitation-hardened high-entropy alloy with outstanding

tensile properties. Acta Materialia. 2016;**102**:187-196

[101] Manivasagam G, Suwas S. Biodegradable Mg and Mg based alloys for biomedical implants. Materials Science and Technology. 2014;**30**:515-520

[102] Zhang Y, Zuo TT, Tang Z, Gao MC, Dahmen KA, Liaw PK, et al. Microstructures and properties of high-entropy alloys. Progress in Materials Science. 2014;**61**:1-93

[103] Cantor B, Chang ITH, Knight P, Vincent AJB. Microstructural development in equiatomic multicomponent alloys. Materials Science and Engineering. 2004:213-218

[104] Wang WR, Wang WL, Wang SC, Tsai YC, Lai CH, Yeh JW. Effects of Al addition on the microstructure and mechanical property of AlxCoCrFeNi high-entropy alloys. Intermetallics. 2012;**26**:44-51

[105] Maiti S, Steurer W. Structural-disorder and its effect on mechanical properties in single-phase TaNbHfZr high-entropy alloy. Acta Materialia. 2016;**106**:87-97

[106] Mohanty S, Maity T, Mukhopadhyay S, Sarkar S, Gurao N, Bhowmick S, et al. Powder metallurgical processing of equiatomic AlCoCrFeNi high entropy alloy: Microstructure and mechanical properties. Materials Science and Engineering A. 2017;**679**:299-313

[107] Zhao Y, Yang Y, Lee C-H, Xiong W. Investigation on phase stability of AlxCo0.2Cr0.2Ni0.2Ti0.4−x high entropy alloys. Journal of Phase Equilibria and Diffusion. 2018;**39**(5):610-622

[108] Chen M-R, Lin S-J, Yeh J-W, Chen S-K, Huang Y-S, Tu C-P. Microstructure and properties of Al0. 5CoCrCuFeNiTix (x = 0-2.0) high-entropy alloys. Materials Transactions. 2006;**47**(5):1395-1401

[109] Davis JR. Alloying: Understanding the Basics. Ohio, USA: ASM International; 2001

[110] Tundermann JH, Tien JK, Howson TE, UB Staff. Nickel and nickel alloys. Kirk-Othmer Encyclopedia of Chemical Technology. 2000:1-19

[111] Bide T, Hetherington L, Gunn G. Nickel. British Geological Survey; 2008

[112] Moutarlier V, Neveu B, Gigandet MP. Evolution of corrosion protection for sol-gel coatings doped with inorganic inhibitors. Surface and Coatings Technology. 2008;**202**(10):2052-2058

[113] Tong C. Advanced materials enable energy production from fossil fuels. In: Introduction to Materials for Advanced Energy Systems. Springer; 2019. pp. 171-230